Effective-medium approximation for composite media: Realizable single-scale dispersions

S. Torquato[a] and S. Hyun
Princeton Materials Institute and Department of Chemistry, Princeton University, Princeton, New Jersey 08544

(Received 21 September 2000; accepted for publication 6 November 2000)

It is known that the popular effective medium approximation (EMA) for the effective conductivity σ_e of a composite is exactly realizable by certain multiscale hierarchical microstructures. We have found a class of periodic, single-scale dispersions that achieve the EMA function at a given phase conductivity ratio for a two-phase, two-dimensional composite over all volume fractions. Moreover, to an excellent approximation (but not exactly), the same structures realize the EMA for almost the entire range of phase conductivities and volume fractions. The inclusion shapes are given analytically by the generalized *hypocycloid*, which in general has a nonsmooth interface. To find these structures, we utilized target optimization techniques and a theorem concerning the spectral function. © *2001 American Institute of Physics.* [DOI: 10.1063/1.1336523]

I. INTRODUCTION

The determination of the effective properties of composites continues to be an active area of research. There are a variety of techniques that have been used to estimate the effective properties, including approximate methods, rigorous bounding techniques, and numerical methods.

Bruggeman's symmetric effective-medium approximation (EMA) for the effective conductivity σ_e of an isotropic two-phase composite[1] remains a popular self-consistent approximation. Analogous expressions also exist for the effective elastic moduli of composites[2] and are equally popular. For the case of a two-phase, two-dimensional, isotropic composite, the EMA formula for σ_e is given by

$$\phi_1\left(\frac{\sigma_e-\sigma_1}{\sigma_e+\sigma_1}\right)+\phi_2\left(\frac{\sigma_e-\sigma_2}{\sigma_e+\sigma_2}\right)=0, \tag{1}$$

where ϕ_i and σ_i are the volume fraction and conductivity of phase i, respectively. Note that relation (1) is invariant to the simultaneous interchange $\sigma_1 \leftrightarrow \sigma_2$ and $\phi_1 \leftrightarrow \phi_2$.

The EMA expression (1) is derived by embedding a single circular inclusion in a homogeneous medium whose effective conductivity σ_e is the unknown to be calculated and determining σ_e in a self-consistent fashion. This relation is analytical because it relies on the known exact field solution for a single circular inclusion of one conductivity in an infinite matrix of another conductivity. Because of its simplicity, it tends to be liberally and often incorrectly applied to various microstructures, including dispersions of identical circular disks at arbitrary volume fractions. Moreover, it has been criticized because it predicts a spurious percolation threshold ($\phi_2=1/2$) for dispersions of identical circular disks.

Interestingly, Milton showed that the EMA expression is exactly realized by granular aggregates of the two phases such that spherical grains (in any dimension) of comparable size are well separated with self-similarity on all length scales.[3] In light of this result, it is clear why the EMA formula breaks down when applied to dispersions of identical circular inclusions. Since the EMA formula (1) is realizable, it must satisfy the general phase–interchange relation[4]

$$\sigma_e(\sigma_1,\sigma_2)\sigma_e(\sigma_2,\sigma_1)=\sigma_1\sigma_2, \tag{2}$$

where $\sigma_e(\sigma_1,\sigma_2)$ and $\sigma_e(\sigma_2,\sigma_1)$ are the effective conductivities of the original isotropic composite and the one with the same microstructure but with the phases interchanged. Relation (2) applies to any two-phase, two-dimensional isotropic composite.

An interesting question is the following: Can the EMA formula be realized by simple structures with a single length scale? The discovery of such structures would be of fundamental value and would lend new insight into the applicability of the EMA formulation. We know from the derivation of (1) that dilute distributions of circular inclusions of phase 2 (phase 1) in a matrix of phase 1 (phase 2) realize the EMA formula when $\phi_2 \to 0$ ($\phi_1 \to 1$). However, at arbitrary volume fractions, it is not known whether single-scale structures achieve (1) and, if so, whether one can find such structures that are independent of the phase contrast ratio σ_2/σ_1.

In determining whether there are single-scale structures that achieve an effective conductivity function, there are two different levels of realizability, in increasing levels of difficulty in realization:

(1) Finding a microstructure that matches the effective conductivity for a given phase contrast ratio σ_2/σ_1 for all volume fractions; and

(2) finding a microstructure that matches the entire conductivity function, i.e., with a microstructure that is independent of σ_2/σ_1 (or independent of the frequency if one is considering the quasistatic response).

In this article, we show that for the EMA formula (1), there is a special two-dimensional dispersion of inclusions characterized by a single length that achieves the first goal and, to an excellent approximation, achieves the second goal

[a]Corresponding author; Electronic mail: torquato@princeton.edu

for almost all phase conductivities and volume fractions. The inclusion shapes are given analytically by the generalized *hypocycloid*. We arrive at this result by formulating the task as a target optimization problem and then solving it by a two-step process. In the first step, we utilize the topology optimization method to suggest the basic topological and geometrical features of the dispersions. This process and a theorem leads to a proposed analytical shape (generalized hypocycloid) for the inclusions whose free parameters are found to match the EMA effective conductivity function (1) via shape optimization.

II. TARGET OPTIMIZATION

We will restrict ourselves to periodic media. However, for such composites, there are no exact techniques that can yield closed-form analytical solutions of the effective conductivity for inclusions of simple shape (e.g., circles) at arbitrary volume fractions, let alone inclusions of arbitrary shape. Thus, the search for single-scale structures that attain (1) at arbitrary volume fractions must ultimately be carried out numerically.

The target optimization procedure introduced by us recently[5] is a means of finding composite microstructures with targeted properties under specified constraints. For the problem at hand, the objective function Φ for the target optimization problem is given by a least-squares form involving the effective property σ_e and a target property σ_0, which we take to be given by the EMA relation (1). Thus, the optimization problem is defined as follows:

$$\text{minimize: } \Phi=(\sigma_e-\sigma_0)^2 \tag{3}$$

$$\text{subject to: fixed volume fraction}$$

$$\text{and prescribed symmetries.}$$

An initial microstructure is allowed to evolve to the targeted state by minimizing the objective function Φ. Various existing optimization procedures can be used to solve the above target problem, including the *topology* optimization method[6,7] and *shape* optimization procedure.[6]

To begin, we use an adaptation of the topology optimization procedure for target optimization[5] to determine: (i) whether single-scale structures that realize (1) can be found and (ii) if so, what are the topologies and geometries of the structures suggested by the technique. The design domain is the periodic square unit cell and is initialized by discretizing it into 14 400 square finite elements. The optimization procedure proceeds sequentially. At each step in the evolution of the target optimization procedure, the local fields are found using finite elements and then averaged to yield the effective conductivity. This is followed by changes in material type of each of the finite elements, based on sensitivities of the objective function and constraints. This process continues until the objective function is minimized.

We simulated a very wide range of volume fractions ($\phi_2=0.1-0.9$) starting from random initial guesses. We imposed reflection symmetry about the horizontal and vertical axes and studied a wide range of values of the phase contrast ratio σ_2/σ_1. Indeed, the algorithm finds single-scale structures with targeted effective conductivities that are in very good agreement with the EMA values that (within the numerical accuracy of the topology optimization method) are independent of the ratio σ_2/σ_1. These structures possess phase-inversion symmetry, i.e., the morphology of phase 1 at volume fraction ϕ_1 is the same as the morphology of phase 2 when the volume fraction of phase 1 is $1-\phi_1$. Thus, we need only focus on the range $0\leqslant\phi_2\leqslant 1/2$.

We verified that as ϕ_2 approaches zero, phase 2 approaches a circular inclusion. On the other hand, at $\phi_1=\phi_2=1/2$, the EMA formula reduces to the geometric-mean formula

$$\sigma_e=\sqrt{\sigma_1\sigma_2}, \tag{4}$$

and our algorithm finds the regular checkerboard arrangement. Thus, at $\phi_1=\phi_2=1/2$, the square unit cell contains a smaller square (phase 2), rotated at 45°, whose corners just touch the sides of the unit cell. The regular checkerboard is known to be one of the structures that exactly achieves (4), independent of the ratio σ_2/σ_1. From the phase–interchange relation (2), it is seen that the geometric-mean formula $\sigma_e=\sqrt{\sigma_1\sigma_2}$ is exact for any two phase, two-dimensional composite whose phase topologies are statistically equivalent. This class encompasses a variety of different composites, including the regular checkerboard, other regular arrangements and the random checkerboard. The regular checkerboard is found because of the symmetries that we impose, unit cell that we employ, and the size of the ''filter'' that we use to avoid local minima.[7] Note that conduction is dominated by transport through the ''necks'' (corner points) connecting the conducting phase. Indeed, this is consistent with the fact that EMA structures have a percolation threshold $\phi_2=1/2$ in the limits $\sigma_2/\sigma_1\to\infty$ or $\sigma_2/\sigma_1\to 0$.

Therefore, for our special dispersions that realize the EMA formula, phase 2 deforms from a very small circular inclusion arranged in a regular checkerboard pattern in a matrix of phase 1 when $\phi_2\to 0$ to large conducting and nonconducting square inclusions of identical sizes arranged on a regular checkerboard when $\phi_2=1/2$. At intermediate volume fractions, the inclusion shapes are quite interesting. At $\phi_2\approx 0.1$, the inclusions are square-like in shape. At still higher values of ϕ_2, the inclusions are star shaped with four points. For example, Fig. 1 shows a 2×2 cell at $\phi_2=0.3$ and $\sigma_2/\sigma_1=100$. The inclusion eventually becomes a square at $\phi_2=1/2$.

III. SHAPE OPTIMIZATION

Although the topology optimization technique captures the salient topological and geometrical features of the microstructures, it is difficult for this method to yield nonsmooth interfaces (hinted at in Fig. 1) when using square finite elements in the digitization process. However, a theorem due to Bergman[8] states that the interface of a periodic composite (not at percolation) must be nonsmooth if the spectrum of the conductivity function is continuous. Now since it is known

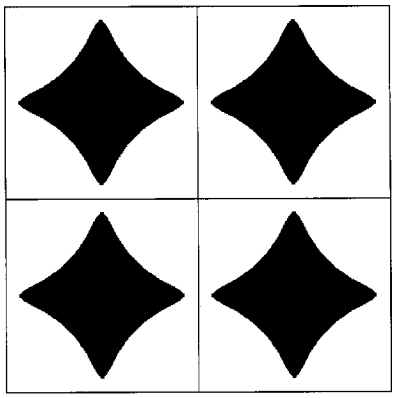

FIG. 1. Periodic medium (2×2 unit cells) that realizes the EMA relation (1) for $\phi_2=0.3$ and $\sigma_2/\sigma_1=100$ as suggested by the target optimization procedure. Phases 1 and 2 are the white and black phase, respectively.

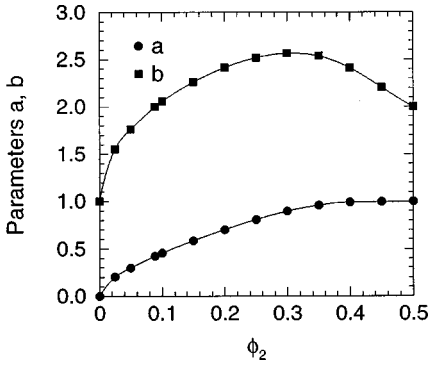

FIG. 2. The dimensionless parameters a and b vs the volume fraction ϕ_2 of phase 2 in the range $0\leqslant\phi_2\leqslant1/2$ for the EMA relation (1). The filled circles and squares are computed data and the solid curves are spline fits of the data. Because of phase-inversion symmetry, the values of a and b for $1/2\leqslant\phi_2\leqslant1$ are obtained from the above curves and the relations $a(\phi_2)=a(1-\phi_2)$ and $b(\phi_2)=b(1-\phi_2)$.

that the EMA relation (1) has a continuous (branch cut) spectrum,[9] then, for volume fractions in the range $0\leqslant\phi_2<1$, the interfaces must be nonsmooth.

An inclusion shape that satisfies the above mentioned basic topological and geometrical features of the target optimization results but whose boundary is nonsmooth for $0\leqslant\phi_2<1$ is the generalized hypocycloid. This shape is defined in the x-y plane by the equation

$$x^{2/b}+y^{2/b}=a^{2/b}, \tag{5}$$

where a and b are dimensionless parameters and all distances (x, y, and a) are given in units of the cell length. The special cases $b=1$, 2, and 3 specifies the circle, square, and four-cusped hypocycloid,[10] respectively. The volume fraction of this periodic composite is given by

$$\phi_2=\int_0^a (a^{2/b}-x^{2/b})^{b/2}dx. \tag{6}$$

To examine whether this proposed shape realizes the EMA formula, we use the shape optimization procedure, except here we utilize the boundary-element method[11] to determine the effective conductivity. The boundary-element method is highly accurate, even for nonsmooth boundaries, because the interface is discretized into line elements.

Before determining the optimum values of a and b, we first checked the accuracy of boundary-element method procedure against known results for the conductivity σ_e of square inclusions. Mortola and Steffe[12] have conjectured that a square array of oriented square inclusions (whose principal axes coincide with the coordinate frame) at an inclusion volume fraction $\phi_2=1/4$ is exactly given by

$$\frac{\sigma_e}{\sigma_1}=\sqrt{\frac{\sigma_1+3\sigma_2}{3\sigma_1+\sigma_2}}. \tag{7}$$

Subsequently, Obnosov[13] proved this conjecture to be rigorously true. We carried out boundary-element calculations for this special case for a number of phase contrast ratios, including the infinite-contrast cases $\sigma_2/\sigma_1=0$ and $\sigma_2/\sigma_1=\infty$, and found agreement with the exact result [Eq. (7)] up to five significant figures for the typical resolutions used. We also computed σ_e for periodic arrays of square inclusions arranged in a checkerboard pattern (whose principal axes are oriented at 45° with respect to the coordinate frame) for a wide range of volume fractions and phase contrast ratios. We compared these results to corresponding results of Hui and Ke-da[14] who computed σ_e by solving numerically the truncated set of linear equations for the potential. Our results agree with their results up to at least four significant figures for all volume fractions. The accuracy of our estimates of σ_e for all of the previous examples are consistent with an independent error analysis which we will discuss.

We now return to the determination of the parameters a and b that specify the generalized hypocycloid shape (5). For constant values of the volume fraction ϕ_2, we see from Eq. (6) that the parameter a uniquely determines b and vice versa. By moving along lines of constant ϕ_2 by varying a, we seek to ascertain whether the effective conductivity function so determined intersects the EMA value for a fixed phase contrast ratio σ_2/σ_1. Thus, the problem is reduced to determine whether the objective function (2) can be made to be exactly zero, i.e., σ_e is given by the EMA formula (1). For the boundary element calculation, we used at least 3000 boundary elements. However, we refined the elements near the cusps for the generalized hypocycloids. This was especially necessary for the cases $\phi_2\geqslant0.4$ in which extremely narrow necks existed between neighboring cusps. For example, at $\phi_2=0.45$, the size of refined elements near the cusps is less than 10^{-7} of the domain size. This refinement of the elements enhanced the accuracy significantly in that region.

We first examined the infinite phase-contrast case $\sigma_2/\sigma_1=0$ for $\phi_2<1/2$.[15] We found that, within the accuracy of the BEM technique, the generalized hypocycloids realize the EMA function (1). The resulting EMA values of a and b are plotted in Fig. 2 as a function of the volume fraction for $0\leqslant\phi_2\leqslant1/2$. Table I gives the numerical values for a and b as well as the corresponding effective conductivities along with conservative error estimates based on many different boundary-element meshes. The values of a and b for $1/2\leqslant\phi_2\leqslant1$, are obtained from Fig. 2 (or Table I) and the rela-

TABLE I. Values of the hypocycloid parameters a and b corresponding to the EMA formula (1) for infinite-contrast case $\sigma_2/\sigma_1=0$ for different inclusion volume fractions. The computed effective conductivities (along with error bars) are compared to the values given by the EMA formula (1).

ϕ_2	a	b	σ_e/σ_1 (hypocycloid)	σ_e/σ_1 (EMA)
0.02500	0.20063	1.54968	$0.94996\pm5\times10^{-5}$	0.95000
0.05000	0.29844	1.76404	$0.89997\pm5\times10^{-5}$	0.90000
0.08878	0.42137	2.00000	$0.82242\pm5\times10^{-5}$	0.82245
0.10000	0.45352	2.05581	$0.79997\pm5\times10^{-5}$	0.80000
0.15000	0.58555	2.26236	$0.69998\pm5\times10^{-5}$	0.70000
0.20000	0.70373	2.41572	$0.59998\pm5\times10^{-5}$	0.60000
0.25000	0.80895	2.52076	$0.50001\pm5\times10^{-5}$	0.50000
0.30000	0.89740	2.56810	$0.40002\pm5\times10^{-5}$	0.40000
0.35000	0.96156	2.53804	$0.29998\pm1\times10^{-4}$	0.30000
0.40000	0.99383	2.41045	$0.2000\pm1\times10^{-4}$	0.20000
0.45000	0.99996	2.20761	$0.1001\pm5\times10^{-4}$	0.10000

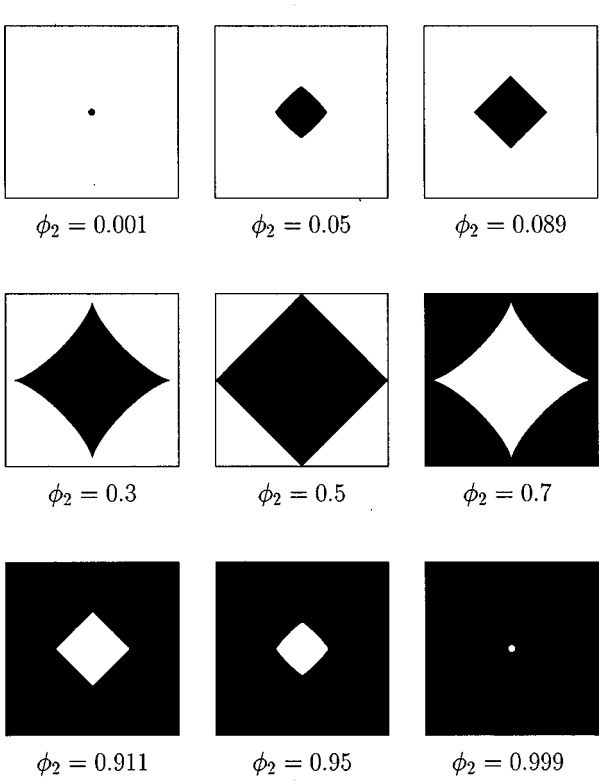

FIG. 3. Unit cells of generalized hypocycloidal inclusions in a matrix that realize the EMA relation (1) for selected values of the volume fraction in the range $0<\phi_2<1$. Phases 1 and 2 are the white and black phase, respectively. To emphasize the phase-inversion symmetry property, we have shifted the locations of the unit cells for $\phi_2>1/2$.

tions $a(\phi_2)=a(1-\phi_2)$ and $b(\phi_2)=b(1-\phi_2)$, by virtue of phase-inversion symmetry. As expected, $a=0$ and $b=1$ for $\phi_2=0$ and $\phi_2=1$, since the circle is recovered in these limits. The special cases of square inclusions occur at three different volume fractions: $\phi_2=0.088\,78$ ($a=0.421\,37$, $b=2$), $\phi_2=1/2$ ($a=1$, $b=2$) and $\phi_2=0.9112$ ($a=0.421\,37$, $b=2$).

The corresponding unit cells of inclusions in a matrix for selected values of the volume fraction in the range $0<\phi_2<1$ are shown in Fig. 3. We can now see precisely how the circle at $\phi_2=0$ transforms to a small square at $\phi_2=0.089$, which in turn transforms to the large square at $\phi_2=1/2$. The nonsmoothness of the interface is apparent for virtually all volume fractions and explains why the EMA formula cannot be applied to dispersions of identical circular inclusions under general conditions.

To determine whether the generalized hypocycloidal dispersions realized the EMA formula independent of the phase-contrast ratio, we carried out two different studies. In the first study, we computed the effective conductivity using the microstructure (Table I) for different finite phase contrast ratios ($\sigma_2/\sigma_1=0.9$, 0.5, 0.2, 10^{-1}, 10^{-2}, 10^{-4}, and 10^{-6}) and compared the results to the EMA values. We found that, to an excellent approximation, the computed effective conductivities matched the EMA values, except for the case of $\phi_2=0.45$ and $\sigma_2/\sigma_1=10^{-2}$. At the smallest volume fraction ($\phi_2=0.025$), we found perfect agreement (within numerical accuracy), independent of σ_2/σ_1. The error increases as the volume fraction is increased up to $\phi_2=0.45$ and eventually goes to zero at $\phi_2=1/2$, where of course our dispersion exactly achieves the EMA formula. For $\phi_2=0.088\,78$, 0.2, and 0.3, the largest errors (occurring at $\sigma_2/\sigma_1=10^{-1}$) are 0.015%, 0.11%, and 0.83%, respectively. For $\phi_2=0.4$ and $\phi_2=0.45$, the largest errors (occurring at $\sigma_2/\sigma_1=10^{-2}$) are 2.9% and 8.3%, respectively. However, in these two cases, the errors for other phase contrasts appreciably smaller than their maximum values.

In the second study, we carried out calculations to ascertain the best values of the parameters a and b for other phase contrast ratios. Importantly, we found that we were always able to find generalized hypocycloidal shapes for all volume fractions, regardless of the ratio σ_2/σ_1 and with the same accuracy reported above for $\sigma_2/\sigma_1=0$. However, we found that the parameters a and b changed slightly from the values reported in Table I with errors comparable to those found in the first study.

Another way to show that the generalized hypocycloidal dispersions cannot exactly realize the EMA relation for all ϕ_2 and σ_2/σ_1 is to appeal to the spectral properties of the conductivity function. Hetherington and Thorpe[16] have studied the spectral properties of the effective conductivity of dilute dispersions of regular polygonal inclusions to first order in ϕ_2. Specifically, they determined that a polygonal corner having an included angle of θ will produce a branch cut of the conductivity function extending between conductivity ratios of $\theta/(\theta-2\pi)$ and $(\theta-2\pi)/\theta$. However, this result extends to nondilute concentrations of arrays of polygonal inclusions because near the branch cut all the power dissipation essentially occurs within an infinitesimal distance away from the corner point.[17] For the case of a square ($\theta=\pi/2$), the branch cut occurs between $-1/3$ and -3. Indeed, we see that the Mortola–Steffe analytical formula (7) for periodic arrays of squares at $\phi_2=1/4$ has such a branch cut between these two points.

For the generalized hypocycloidal dispersion, the special case of square inclusion occurs, among other volume fractions, at $\phi_2=0.088\,78$. We can check whether the branch cut between $-1/3$ and -3 for this volume fraction is consistent with the branch cut of the EMA conductivity function (1) which extends between the following two points:[9]

$$\frac{(\phi_1-\phi_2)^2-2\pm 4\sqrt{\phi_1\phi_2}}{(\phi_1-\phi_2)^2}. \tag{8}$$

At $\phi_2=0.088\,78$, this relation predicts a branch cut between $-0.274\,82$ and -3.6388, which we see is inconsistent with the branch cut for square inclusions.

IV. DISCUSSION AND CONCLUSIONS

To summarize, periodic arrays of generalized hypocycloidal inclusions arranged in a checkerboard pattern achieve (within numerical accuracy) the EMA formula (1) for all volume fractions for a given ratio σ_2/σ_1. Moreover, the same structures achieve this conductivity function, to an excellent approximation, for almost all phase conductivities and volume fractions. At dilute inclusion concentrations, our single-scale structures appear to correspond exactly to the EMA formula for any σ_2/σ_1.

If the last point is true, then the nonsmoothness of the generalized hypocycloidal inclusions is already reflected in the expansion of the EMA relation through second order in ϕ_2:

$$\frac{\sigma_e}{\sigma_1}=1+2\left(\frac{\sigma_2-\sigma_1}{\sigma_2+\sigma_1}\right)\phi_2+\frac{4\sigma_2}{\sigma_1+\sigma_2}\left(\frac{\sigma_2-\sigma_1}{\sigma_2+\sigma_1}\right)^2\phi_2^2+\mathcal{O}(\phi_2^3). \tag{9}$$

This is to be contrasted with the corresponding expansion for periodic arrays of circles:[18]

$$\frac{\sigma_e}{\sigma_1}=1+2\left(\frac{\sigma_2-\sigma_1}{\sigma_2+\sigma_1}\right)\phi_2+2\left(\frac{\sigma_2-\sigma_1}{\sigma_2+\sigma_1}\right)^2\phi_2^2+\mathcal{O}(\phi_2^3). \tag{10}$$

Through first order in ϕ_2, both expressions agree since in each case this corresponds to noninteracting circular inclusions. The two expansions differ at the second order term because the inclusion (presumably corresponding to the hypocycloid) is already noncircular.

The fact that the EMA relation is realizable (albeit approximately) by single-scale structures raises many interesting questions and issues. Are the generalized hypocycloidal inclusions that we have found to attain the EMA relation unique? We believe the answer to this question is in the negative. For example, if we had chosen a different underlying lattice (e.g., triangular or hexagonal), we suspect that the EMA relation would be realizable by different inclusion shapes. The question of the realizability by single-scale structures of the corresponding EMA expression in three dimensions and of the EMA formulas for the effective elastic moduli is clearly fertile ground. The three-dimensional problems, however, are much more challenging because both phases can be connected.

Our work raises a more general question in the theory of composites: Can *any admissible* effective conductivity function be realized by single-scale structures? It is known that certain multiscale laminates can realize any conductivity function of two-dimensional, two-phase composites.[19] Our work suggests that single-scale structures cannot exactly match any conductivity function. However, finding single-scale structures that approximately realize an effective property function is practically important since such structures can be fabricated and therefore this less ambitious goal is still very attractive. All of these questions and issues will be addressed in future studies.

ACKNOWLEDGMENTS

The authors gratefully acknowledge many invaluable discussions with G. W. Milton. This work was supported by the Office of Naval Research under Grant No. N00014-00-1-0438.

[1] D. Bruggeman, Ann. Phys. (Leipzig) **24**, 636 (1935).
[2] B. Budiansky, J. Mech. Phys. Solids **13**, 223 (1965); R. Hill, *ibid.* **13**, 213 (1965).
[3] G. W. Milton, in *Physics and Chemistry of Porous Media*, edited by D. L. Johnson and P. N. Sen (AIP, New York, 1984); G. W. Milton, Commun. Math. Phys. **99**, 463 (1985).
[4] J. B. Keller, J. Math. Phys. **5**, 548 (1964); K. S. Mendelson, J. Appl. Phys. **46**, 917 (1974).
[5] S. Hyun and S. Torquato, J. Mater. Res. **16**, 280 (2001).
[6] M. P. Bendsøe, *Methods for the Optimization of Structural Topology* (Springer, Berlin, 1995).
[7] O. Sigmund and S. Torquato, J. Mech. Phys. Solids **45**, 1037 (1997).
[8] D. J. Bergman, in *Les Méthods d'Homogénéisation: Théorie et Applications en Physique* (Cours de l'Ecole d'Eté d'Analyse Numeriqué, Eyrolles, Paris, 1985).
[9] D. J. Bergman, Phys. Reports **43**, 377 (1978).
[10] The standard hypocycloid ($x^{2/3}+y^{2/3}=a^{2/3}$) is a curve described by a point P on a circle of radius $a/4$ as it rolls on the inside of a circle of radius a.
[11] C. A. Brebbia, J. C. F. Telles, and L. C. Wrobel, *Boundary Element Techniques* (Springer, Berlin, 1984).
[12] S. Mortola and S. Steffè, Rendiconti **78**, 77 (1985).
[13] Y. V. Obnosov, SIAM J. Appl. Math **59**, 1267 (1999).
[14] L. Hui and B. Ke-da, Phys. Rev. B **46**, 9209 (1992).
[15] The case $\phi_2=1/2$ does not have to be considered since we already know the regular checkerboard exactly achieves $\sqrt{\sigma_1\sigma_2}$, independent of σ_2/σ_1.
[16] J. H. Hetherington and M. F. Thorpe, Proc. R. Soc. London, Ser. A **438**, 591 (1992).
[17] G. W. Milton (private communication).
[18] W. T. Perrins, D. R. McKenzie, and R. C. McPhedran, Proc. R. Soc. London, Ser. A **369**, 207 (1978).
[19] G. W. Milton, in *Advances in Multiphase Flows and Related Problems*, edited by G. Papanicolaou (SIAM, Philadelphia, 1986). It is an open question whether all conductivity functions of three-dimensional composites are attainable by multiscale laminates.